Scientific Research Publishing

Advances in Chemical Engineering and Science, 2017, 7, 215-227
http://www.scirp.org/journal/aces
ISSN Online: 2160-0406
ISSN Print: 2160-0392

Performance Evaluation of Palm Kernel Shell Adsorbents for the Removal of Phosphorus from Wastewater

Akinpelu Kamoru Babayemi

Department of Chemical Engineering, Anambra State University, Uli, Nigeria
Email: akinbabs40@yahoo.com

How to cite this paper: Babayemi, A.K. (2017) Performance Evaluation of Palm Kernel Shell Adsorbents for the Removal of Phosphorus from Wastewater. *Advances in Chemical Engineering and Science*, **7**, 215-227.
https://doi.org/10.4236/aces.2017.72016

Received: November 24, 2016
Accepted: April 21, 2017
Published: April 25, 2017

Abstract

Studies were carried out on Palm Kernel Shell, an agricultural waste available in large quantity in Nigeria, to evaluate its ability to remove phosphorus from wastewater. The adsorbents, which were prepared from Palm Kernel Shells (PKN), were characterized using Fourier Transform Infrared (FT-IR), Energy dispersive *X*-ray (EDX) and Scanning Electron Microscopy (SEM). Batch mode experiments were conducted to study the effects of adsorbent dosage and contact time on phosphorus adsorption. Equilibrium and Kinetic studies of the process were also carried out. Results obtained show that, FT-IR spectrum of the activated carbon displays a number of absorption peaks, reflecting the complex bio-mass structure and a variety of functional groups which explains its improved adsorption behaviour on the colloidal particles. SEM shows the spherical shape of the carbon particles with a wide range of sizes, EDX indicated the constituent elements in the adsorbent in which C and O were found to be the most abundant. Equilibrium data fitted well to the Freundlick and Langmuir models but the data were best described by Langmuir Isotherm model at the temperature of 313 K. Pseudo second order best described the kinetics of the adsorption process. Removal efficiency (*E*%) of 97% was attained within 120 minutes at 50 g/l adsorbent concentration, pH6 and 0.2mm particle size of the adsorbent.

Keywords

Phosphorus, Adsorbent, Activated Carbon, Isotherms, Kinetics, Equilibrium, Adsorption

1. Introduction

Phosphorus pollution is a major problem emanating from natural decomposi-

tion of rocks and minerals, agricultural runoff, erosion and sedimentation, improper disposal of wastes generated especially from indigenous chemical industries such as fertilizers, soap and detergent companies [1].

Phosphorus is a common constituent of agricultural fertilizers, manure and organic wastes in sewage and industrial effluent. It is an essential element for plant life but when there is too much of it in water, it results in the contamination of groundwater and eutrophication of lakes, rivers and canals. Eutrophication results in reductions in aquatic fish and other animal populations as it promotes excessive growth of algae [1] [2]. As the algae die and decompose, high levels of organic matter and the decomposing organism deplete the water of oxygen. Even some algal blooms are harmful to humans because they produce elevated toxins and bacterial growth that can make people sick if they come in contact with the polluted water or consume the contaminated aquatic foods.

Given the severity of environmental impact of phosphorus pollution to our local, national and global communities, it is imperative that a technologically feasible, economically viable and socially acceptable solution be found to solve the problem. Against this background, adsorption process has been adopted using Palm Kernel Shell, a bio degradable non-toxic agricultural waste available in large quantity in Nigeria.

Palm Kernel Shells are the shell fractions left after the nut has been removed in the palm oil mill. In the palm oil value chain, the utilization rate of palm kernel shell is comparatively very low.

2. Materials and Methods

Palm Kernel Shells (PKN) were obtained from Umuoma village, near Anambra State University Campus, Uli. The shells were cleaned and dried in a Memmert oven at 110˚C for 24 hrs. The dried sample was then carbonized in a muffle furnace at a temperature of 800˚C for 3 hrs. The charred material was allowed to cool to room temperature, ground and sieved using 0.2 mm mesh. The sieved 0.2 mm particle size material was weighed and impregnated with 1M H_2SO_4 at the ratio of 1:2 (wt%) for 12 hrs. The impregnated sample was washed with de-ionized water until pH 7.0, filtered and dried in an oven at 110˚C for 24hrs before being packed in an air tight sample bags for use.

Proximate analysis was carried out on the activated PKN to determine the % weight loss, bulk density (g/cm^3), % ash content, iodine number, % volatile matter, % moisture content and % fixed carbon using standard methods [3] [4]. Surface area of the PKN was estimated using Sear's method [5] [6]. PKN was also characterized using: Fourier Transform Infrared to identify the presence of functional groups, Energy dispersive *X*-ray for the identification of the constituent elements and Scanning Electron Microscopy for surface morphologies and pores diameters distribution.

The effluent used in the experiment was prepared by first dissolving 500 g of phosphate rock sample in 1000 cm^3 of de-ionized water. The solution was thoroughly stirred and filtered off the silts, organic matters and insoluble phosphate

rock particles. The filtrate was further diluted with 3000 cm^3 deionized water before it was tested for pH level with digital pH meter and its phosphorous content concentration was measured in UV spectrophotometer set at a wavelength of 650 nm. The initial pH was 2.8 and phosphorus concentration was 373 mg/l.

Batch Adsorption Experiment

1.0 g of PKN was added to 100ml of the synthesized effluent in a conical flask and placed on a magnetic stirrer.

The stirring was done at different temperatures of 30˚C, 35˚C, 40˚C and at different stirring periods (contact time) of 30 mins., 60 mins., 120 mins., 180 mins., 240 mins. and 300 mins. respectively. Upon the completion of each stirring period, the solution was filtered using what man filter paper. The residual concentration of the filtrate was determined using UV-spectrophotometer set at wavelength of 650 nm. The same procedure was repeated for 2.0 g, 3.0 g, 4.0 g and 5.0 g of the adsorbent respectively. Removal efficiency $E\%$ was calculated using Equation (1).

$$E\% = \left[\left(C_o - C_1\right)/C_o\right] \quad (1)$$

where C_o and C_1 are respectively the initial and residual concentrations of phosphorus in the effluent (mg/l).

3. Results and Discussion

Physico-chemical characteristics of PKN derived activated carbon are presented in Table 1.

The surface morphology of the PKN before and after sorption is measured and presented in Plate 1 and Plate 2 respectively. Plate 1 clearly reveals the surface texture of the materials with a wide range of sizes before adsorption. Plate 2 shows the morphological changes with respect to shape and size of the activated carbon after adsorption. It can be clearly observed that, the surface of the activated carbon has been changed into a new shining bulky particles and whitish patches structure.

Table 1. Physico-chemical characteristics of PKN.

Parameters	PKN
Weight loss %	44.79
Bulk density g/cm^3	0.48
Ash content, %	6.33
Iodine number, mg/g	558.06
Volatile matter, %	20.87
Moisture content, %	7.17
Fixed carbon, %	75.28
Surface area, m^2/g	635.73

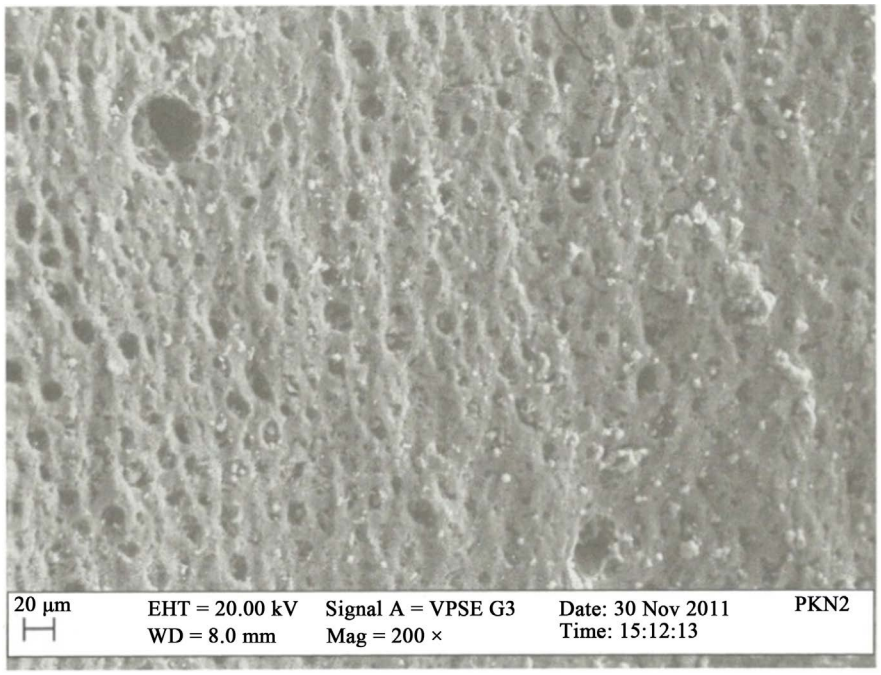

Plate 1. PKN before adsorption

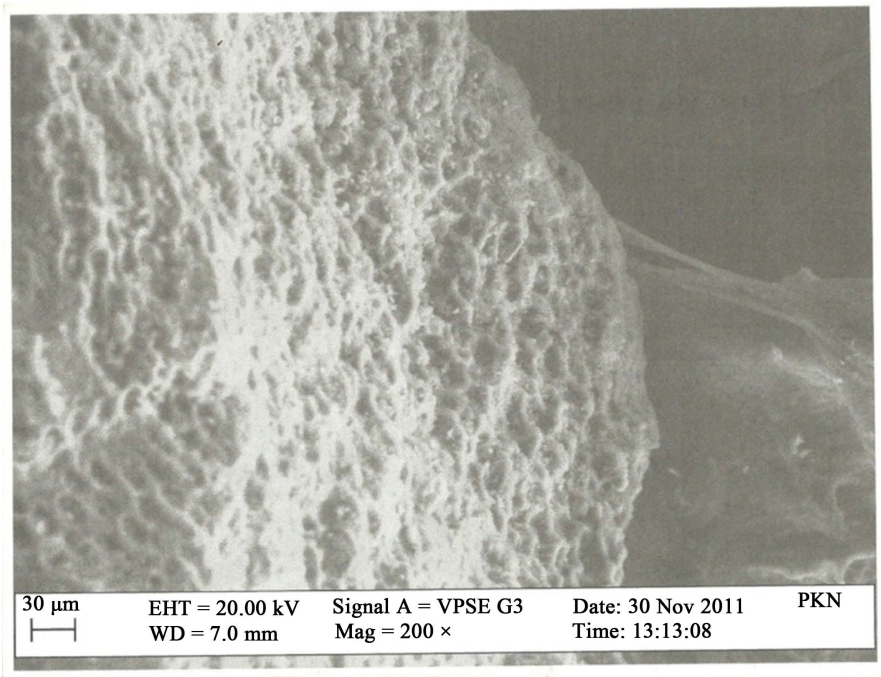

Plate 2. PKN after adsorption.

The qualitative elements composition of the activated carbon was analyzed and presented in Table 2. The EDX patterns for PKN reveals that C and O are the main constituents, an indication of PKN suitability for adsorption process.

FTIR spectrum of the activated PKN displays a number of absorption peaks, reflecting the complex biomass structure. The broad stretching absorption peak between 4288 cm^{-1} and 4638 cm^{-1} indicates C-H group of alkanes and the low

Table 2. Characterization results of PKN using EDX.

Element	App. Conc.	Intensity	*Wt.*%	*Wt.*%. Sigma	Atomic%
C	7.39	0.4037	10.68	0.48	18.67
O	26.27	0.3787	40.49	0.50	53.12
Na	0.53	0.7282	0.42	0.06	0.39
Mg	0.36	0.6991	0.30	0.05	0.26
Al	1.21	0.8162	0.86	0.05	0.67
P	30.97	1.3386	13.50	0.17	9.15
Cl	2.41	0.7985	1.76	0.06	1.04
Ca	54.24	0.9987	31.70	0.32	16.60
Fe	0.39	0.8083	0.28	0.08	0.11
Total				100	

bands of between 509.22 cm^{-1} and 596.99 cm^{-1} indicate C-I aromatic ring vibration as presented in Figure 1.

Effects of Adsorbent Dosage and Contact Time

The removal efficiency of PKN activated with H_2SO_4 as a function of time for varying adsorbent dosages is presented in Figure 2. The figure shows that the removal efficiency of PKN increases very fast within the first 60 mins after which the rate of adsorption began to decrease gradually with time. As the system approaches equilibrium stage between 180 mins and 240 mins, no significant changes were observed in the rate of removal. The sharp increase in removal efficiency at the early stages of adsorption may be due to the availability of the active sites of PKN which were yet to be saturated by the adsorbates [7] However, as the process proceeds most of the available sites get occupied by the adsorbates thereby reducing the possibility of contact between the surface area of the solute ion and the adsorbent [8]. Also, increase in the adsorbent dosage brings about an increase in the fresh and unsaturated adsorbent hence, the increase in the active sites for sorption.

Adsorption Kinetics

Kinetics of sorption describes the solute uptake rate, which in turn governs the residence time of sorption. It is one of the important characteristics in defining the efficiency of sorption. In the present study, the kinetics of the phosphorus removal was carried out to understand the behaviour of PKN.

Pseudo first order kinetic model

The rate constant of adsorption was determined from the Pseudo first order rate expression given by Largergren [9].

$$dq_t/dt = K_1(q_e - q_t) \tag{2}$$

where q_e and q_t (mg/g) are the amounts of phosphorus adsorbed at equilibrium and at time t(mins) respectively and K_1 ($mins^{-1}$) is the rate constant of adsorption. After integration and applying boundary conditions, $t = 0$ to $t = t$ and $q_t = 0$ to $q_t = q_t$, the integrated form of Equation (2) becomes

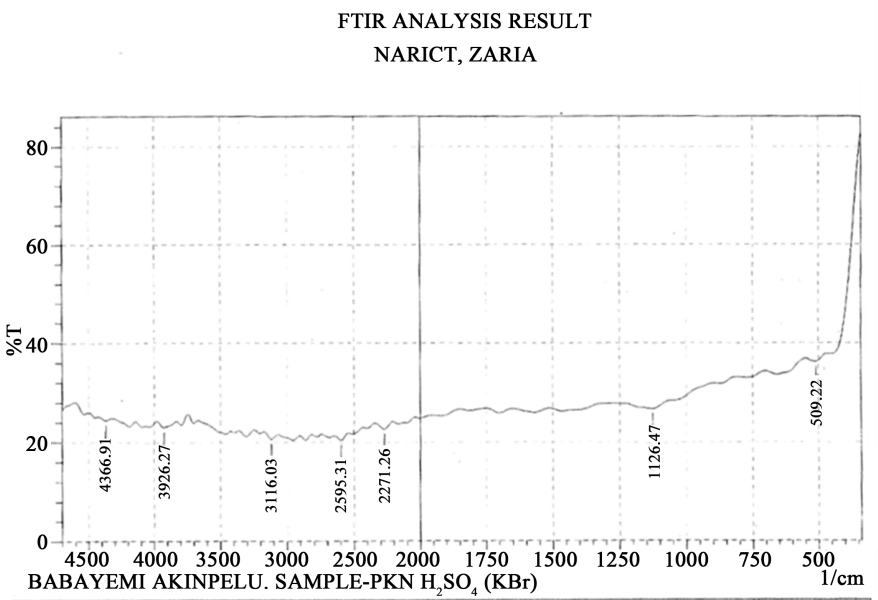

	Peak	Intensity	Corr. Intensity	Base (H)	Base (L)	Area	Corr. Area
1	509.22	36.2365	1.0901	546.84	463.9	35.9633	0.5053
2	1126.47	26.7491	2.4399	1246.06	893.07	191.7454	6.0307
3	2271.26	22.6524	1.3638	2339.73	2209.53	82.2868	1.6074
4	2595.31	20.4506	1.1151	2646.42	2543.23	69.9001	1.1494
5	3118.03	20.6017	1.2528	3172.04	3067.88	70.0469	1.2722
6	3925.27	23.0357	0.3683	3982.17	3909.84	45.4585	0.2516
7	4368.91	24.457	0.5075	4423.89	4329.37	57.3323	0.4178

Figure 1. FTIR spectrum of activated PKN.

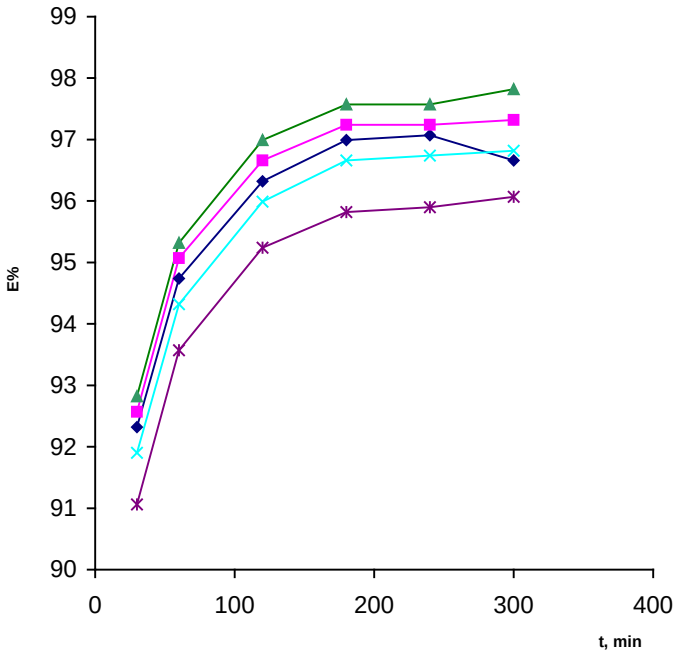

Figure 2. Removal efficiency of PKN activated with H_2SO_4 at different adsorbent concentration.

$$\mathrm{Ln}\left(q_e - q_t\right) = \mathrm{Ln}q_e - K_1 t \tag{3}$$

The rate constants were determined from the slopes and intercept of the plots $\mathrm{Ln}\left(q_e - q_t\right)$ versus t in **Figure 3**.

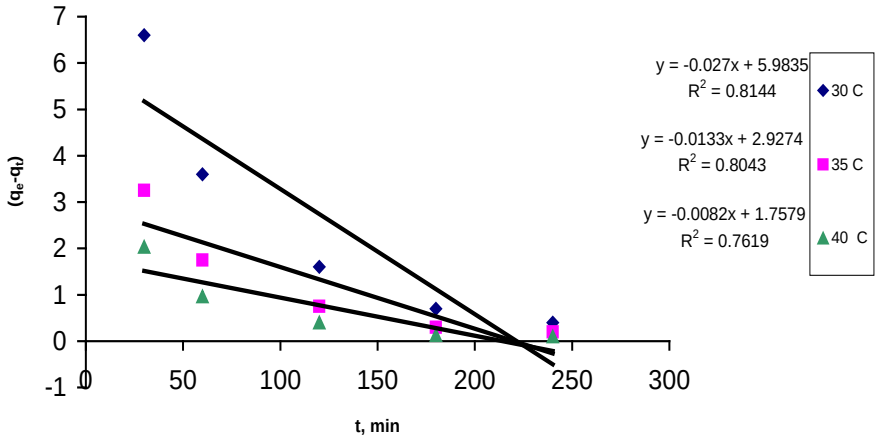

Figure 3. Pseudo-first order plot for the adsorption of phosphorus on PKN.

Pseudo Second Order Kinetic Model

The adsorption Kinetics may also be described by a pseudo second order equation [10]

$$\mathrm{d}q_t/\mathrm{d}t = K_2\left(q_e - q_t\right)^2 \tag{4}$$

Integrating Equation (4) and applying the boundary conditions $t = 0$ to $t = t$ and $q_t = 0$ to $q_t = q_t$ gives

$$1/q_e - 1/q_t = 1/q_e + K_2 t \tag{5}$$

Equation (5) can be rearranged to obtain a linear form

$$t/q_t = 1/K_2 q_e^2 + t/q_e \tag{6}$$

where K_2 is the rate constant of Pseudo second order adsorption ($g \cdot mg^{-1} \cdot min^{-1}$). The plot of $1/q_t$ versus t as presented in Figure 4 gives a linear relationship, from the slope and intercept of which q_e and K_2 can be determined respectively.

Second Order Kinetic Model

The kinetic rate constants for second order kinetic model were evaluated from the plots of $1/(q_e - q_t)$ versus t as presented in Figure 5 and the values of the rate constants are presented in Table 3. The correlation coefficients ($R^2 = 0.9417$) showed that, the data conformed to the second order kinetic model.

Weber and Morris Kinetic Model

Weber and Morris plot was used to investigate the intra-particle diffusion mechanism. The equation used in this case is as follows:

$$q_e = K_d t^{1/2} + \square \tag{7}$$

where □ is Weber and Morris constant and K_d (mg/gmin$^{1/2}$) is intra-particle diffusion rate constant.

K_d and □ are determined from the plots of adsorbate uptake q_t versus the square root of time $t^{1/2}$ as shown in Figure 6 and their values are presented in Table 3.

The deviation of straight lines from the origin indicates that intra-particle transport is not the rate limiting steps and that, pore diffusion is the only con-

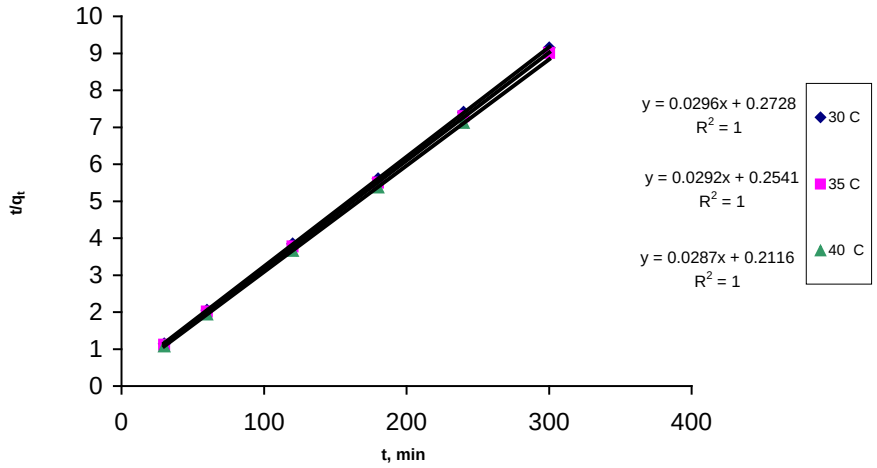

Figure 4. Pseudo second-order plot for the adsorption of phosphorus on PKN.

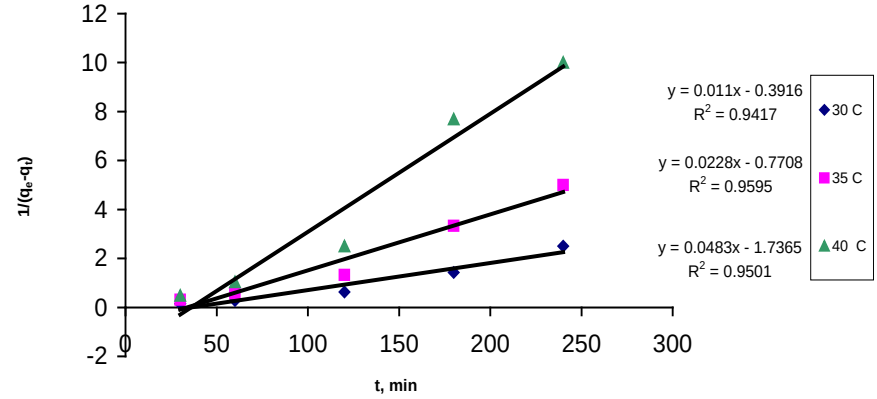

Figure 5. Lagergren second-order plot for the adsorption of phosphorus on PKN.

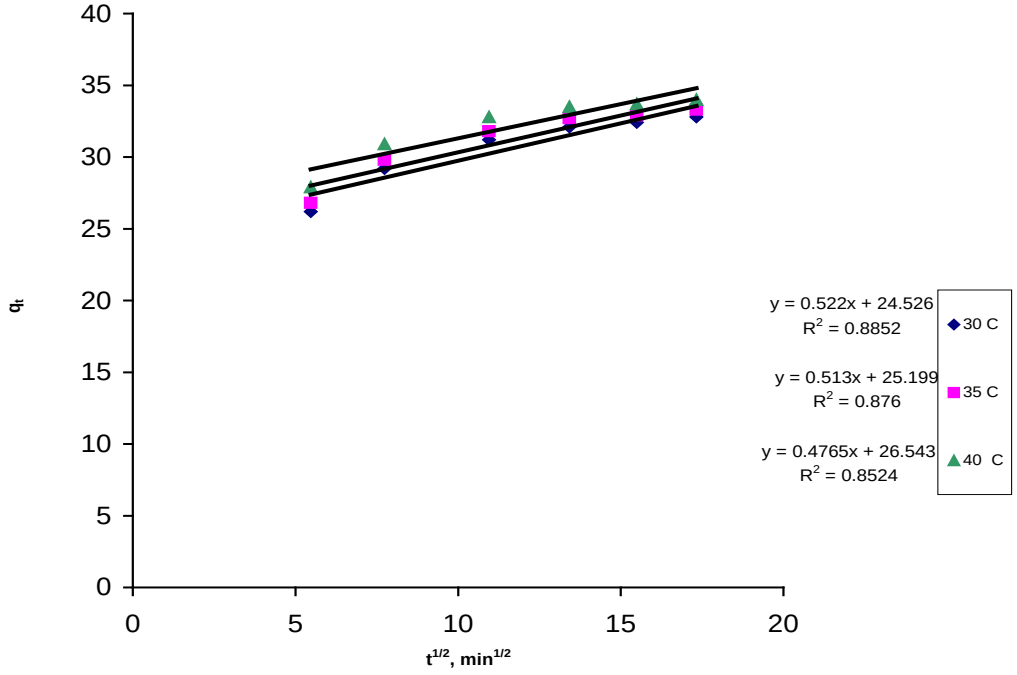

Figure 6. Intraparticle diffusion plot for the adsorption of phosphorus on PKN.

Table 3. Calculated kinetic parameters for the adsorption of phosphorus on PKN at different temperatures.

Kinetic model	Parameter	Temperatures, K			Remarks
		303 K	308 K	313 K	
Pseudo first order	K_1 (min^{-1})	0.0270	0.0133	0.0082	Data did not fit well to the model
	q_e (mg/g)	5.9835	2.9274	1.7579	
	R^2	0.8144	0.8043	0.7619	
Second order	K_2 (mg/g·mn)	0.0110	0.0228	0.0483	Data fitted well to second order kinetic model
	q_e (mg/g)	2.5536	1.2973	0.5759	
	R^2	0.9417	0.9595	0.9501	
Pseudo second order	K_2 (mg/g·min)	0.0032	0.0034	0.0039	Data fitted well at all the three chosen experimental temperatures
	q_e (mg/g)	33.7838	34.2465	34.8432	
	R^2	1.0000	1.0000	1.0000	
Weber and Morris	K_d (mg/g·min^{½})	0.5220	0.5130	0.4765	Data did not conform to Weber and Morris
	□	24.526	25.1990	26.543	
	R^2	0.8852	0.8760	0.8524	
Bhatacharya Venkobachor	K_B (min^{-1})	0.0064	0.0064	0.0340	Data fitted well at the temperature of 313 K
	D_B (m^2/s)	6.48×10^{-12}	6.48×10^{-12}	3.44×10^{-11}	
	R^2	0.8769	0.7206	1.0000	

trolling step and not film diffusion [11] [12] [13].

Bhattacharya-Venkobachor Kinetic Model

Bhattacharya-Venkobachor model is expressed as [14].

$$\mathrm{Ln}\left[1-U_{(t)}\right]=K_B t \tag{8}$$

where,

$$U_{(t)}=\left(C_o-C_t\right)/\left(C_o-C_e\right) \tag{9}$$

The effective diffusion coefficient D_B, is obtained from the equation (Joseph and Philomena, 2011).

$$D_B=\left(K_B r^2\right)/\pi^2 \tag{10}$$

where,

K_B is the Bhattacharya Venkobachor constant (min^{-1})

C_0 is the initial concentration (mg/l)

C_t is the concentration at time t(mg/l)

R is the particle radius

The values of K_B are determined from plots of $\mathrm{Ln}\left[1-U_t\right]$ versus t as presented in **Figure 7**.

Adsorption Isotherms Studies

Adsorption isotherms are characterized by certain constants and described the mathematical relationship between the quantity of adsorbate and concentration of adsorbate remaining in the solution at equilibrium. In this work, Langmuir, Freundlick and Temkin isotherm models have been used to analyze adsorption data at different temperatures.

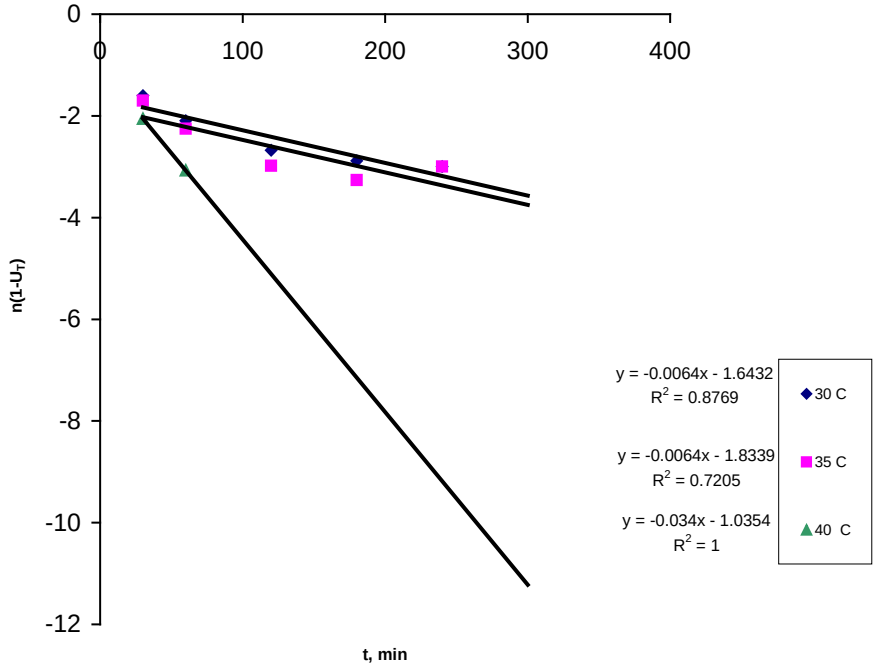

Figure 7. Bhattacharya-Venkobachor plot for the phosphorus on PKN.

Langmuir Isotherm Model

The linearized form of Langmuir Isotherm Model is expressed as:

$$C_e/q_e = 1/K_L q_{\max} + \left[1/q_{\max}\right] C_e \tag{11}$$

where q_e is the equilibrium value of adsorbate per unit mass of adsorbent (mg/g), C_e is the equilibrium concentration of the adsorbate.

Langmuir constants $q_{\max}$ and K_L are determined from the intercepts and slope of the linear plots of C_e/q_e versus C_e as presented in Figure 8.

To confirm the favourability of an adsorption process to Langmuir Isotherm, the essential features of the isotherm can be expressed in terms of a dimensionless constant or separation factor R_L which is expressed as (Babayemi and Onukwuli, 2016; Gueu et al, 2006)

$$R_L = 1/\left(1 + K_L C_o\right) \tag{12}$$

where C_o is the initial adsorbate concentration. The value of R_L indicates whether the isotherm is irreversible ($R_L = 0$), favourable ($0 < R_L < 1$), linear ($R_L = 1$) or unfavourable ($R_L > 1$).

R_L values for phosphorus adsorption on PKN are less than 1 and greater than zero indicating favourable adsorption under the chosen experimental conditions. The values are presented in Table 4.

Freundlick Isotherm Model

The Freundlick adsorption isotherm is expressed as

$$q_e = K_F C_e^{1/n} \tag{13}$$

The linearized form of the above expression is

$$\mathrm{Ln}q_e = \mathrm{Ln}K_F + 1/n\,\mathrm{Ln}C_e \tag{14}$$

Table 4. Isotherm parameters for the adsorption of phosphorus on PKN.

Isotherm	Parameter	Temperatures, K			Remarks
		303 K	308 K	313 K	
Langmuir	q_{max} (mg/g)	4.2158	4.4169	3.8109	$0 < R_L < 1$ shows favourable adsorption of phosphorus on the adsorbents. Data conformed to Langmuir Isotherm
	K_L (1/mg)	0.0196	0.0180	0.0166	
	R_L	0.1203	0.1296	0.1399	
	R^2	0.9509	0.9632	0.9904	
Freundlick	n	0.2328	0.2436	0.2230	$n < 1$ shows favourable adsorption. Data fitted well to Freundlick Isotherm
	K_F (1/g)	2.28×10^{-6}	3.37×10^{-6}	4.9×10^{-7}	
	R^2	0.9476	0.9403	0.9396	
Temkin	B (J/mg)	36.59	39.82	37.77	R^2 values show that data did not fit to Temkin Isotherm
	K_t (1/g)	0.0334	0.0315	0.0276	
	R^2	0.844	0.8123	0.8039	

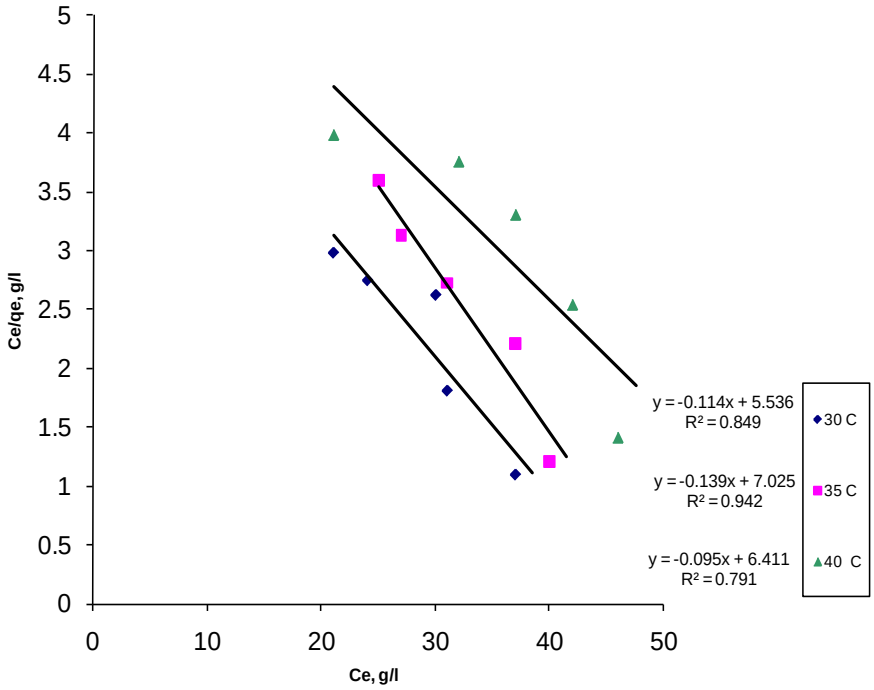

Figure 8. Langmuir isotherm for the adsorption of adsorption of phosphorus on PKN.

The Freundlick constants "n" giving an indication of how favourable the adsorption process is and K_F which is the adsorption capacity of the adsorbent are determined from the slope and intercept of plots of $\mathrm{Ln}q_e$ versus $\mathrm{Ln}C_e$ as presented in **Figure 9**.

Temkin Isotherm Model

The linear form of Temkin Isotherm Model for liquid adsorbate is expressed as:

$$q_e = \left[(RT)/b_T\right]\mathrm{Ln}K_T + \left[(RT)/b_T\right]\mathrm{Ln}C_e \quad (15)$$

Temkin constants K_T and b_T are obtained from the intercepts and slope of the plots of q_e versus $\mathrm{Ln}C_e$ as shown in **Figure 10** and the values are presented in **Table 4**.

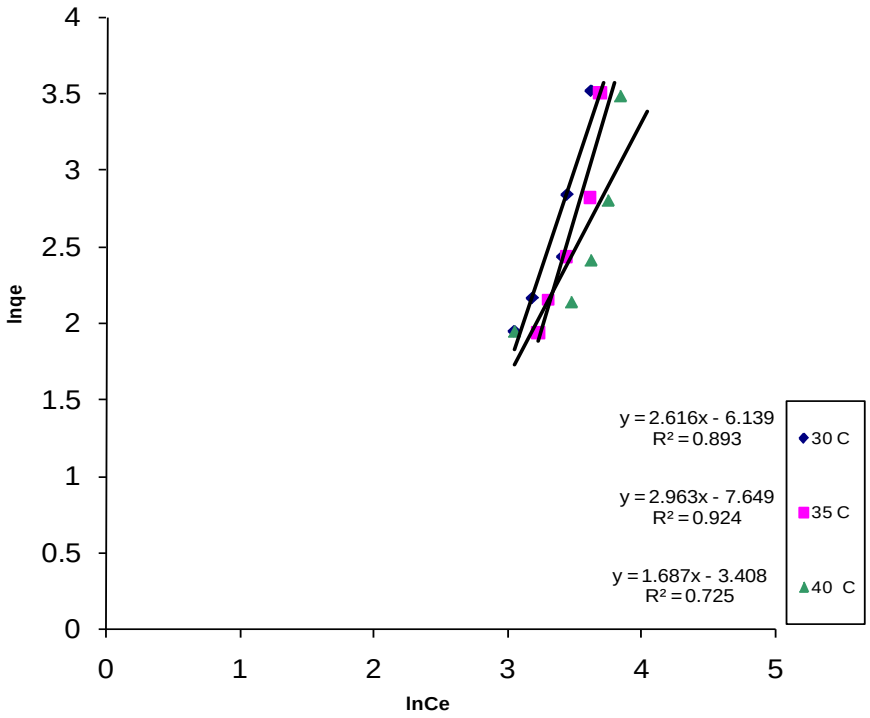

Figure 9. Freundlich isotherm for the adsorption of phosphorus on PKN.

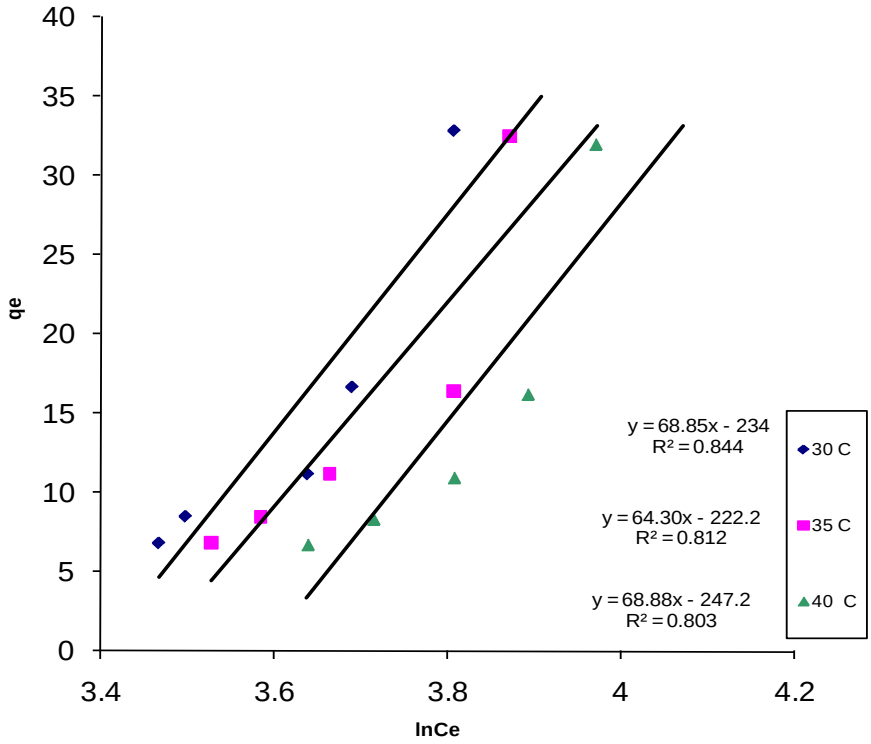

Figure 10. Temkin isotherm for the adsorption of phosphorus on PKN.

4. Conclusions

Activated carbon prepared from palm kernel shell was used to remove up to 97% phosphorus from wastewater through adsorption process. Equilibrium data fit-

ted well to Langmuir and Freundlick Isotherm Models. Kinetics of adsorption was best described by Pseudo Second Order Kinetic Model.

Conclusively, this work has demonstrated that, palm kernel shell, an agricultural waste, non-toxic and bio-degradable material could be used as an effective adsorbent for the removal of phosphorus from wastewater.

References

[1] Babayemi, A.K. (2014) Removal of Phosphorus from Industrial and Synthetic Effluent Using Non-Conventional Coag-Flocculation and Adsorption. Ph.D. Thesis, Nnamdi Azikiwe University, Awka.

[2] Babayemi, A.K. and Onukwuli, O.D. (2015) Kinetics of Adsorption of Phosphorus from Phosphate Containing Synthetic Effluent Using Locally Prepared Bio-Sorbent. *International Journal of Engineering and Technical Research*, **3**, 64-67.

[3] ASTM (1994) American Standard for Testing Materials. West Conshohocken.

[4] AOAC (1989) Official Methods of Analysis. 14th Edition, Association of Official Analytical Chemists, Washington DC.

[5] Alzaydien, A.S. (2009) Adsorption of Methylene Blue from Aqueous Solution onto a Low-Cost Natural Jordanian Tripoli. *American Journal of Environmental Sciences*, **6**, 1047-1058. https://doi.org/10.3844/ajessp.2009.197.208

[6] Babayemi, A.K. and Onukwuli, O.D. (2016) Adsorption Isotherms, Thermodynamics and Statistical Modeling of Phosphate Removal from Aqueous Solution by Locally prepared Bio-Sorbent. *IOSR Journal of Applied Chemistry*, **9**, 46-50.

[7] Babayemi, A.K. (2009) Phosphorus Removal through Adsorption on Locally Prepared Adsorbents. *Journal of Engineering and Applied Sciences*, **5**, 54-57.

[8] Goswani, S. and Ghosh, U.C. (2005) Studies on Adsorption Behaviour of Cr (vi) onto Synthetic Hydrous Stannic Oxide. *Water SA*, **31**, 497-602.

[9] Nwabanne, J.T. and IGbokwe, P.K. (2011) Copper (II) Uptake by Adsorption Using Palmyra Palm Nut. *Advances in Applied Sciences Research*, **2**, 166-175.

[10] Ho, U.S. and Mckay, G. (2000) The Kinetics of Sorption of Divalent Metal Ions onto Sphagnum Moss Flat. *Water Research*, **34**, 735. https://doi.org/10.1016/S0043-1354(99)00232-8

[11] Ahmad, A.A., Hameed, B.H. and Aziz, N. (2008) Adsorption of Direct Dye on Palm Ash; Kinetics and Equilibrium Modeling. *Journal of Hazardous Materials*, **141**, 70-76.

[12] Sivakumar, P. and Palanisamy, P.N. (2009) Adsorption Studies of Basic Red 29 by a Non-Conventional Activated Carbon Prepared from Euphorbia Antiquorum. *International Journal of ChemTech Research*, **1**, 502-510.

[13] Nwabanne, J.T. (2010) Adsorption and Kinetic Modeling of Heavy Metals Uptake from Wastewater Effluents. PhD Thesis, Nnamdi Azikiwe University, Awka.

[14] Gueu, S., Yao, S., Adouby, K. and Ado, G. (2006) Heavy Metals Removal in Aqueous Solution by Activated Carbons Prepared from Coconut Shell and Seed Shell of the Palm Tree. *Journal of Applied Sciences*, **6**, 278-293.